IMPROVEMENTS IN THE RETRIEVAL OF LOW CLOUD MOTION WINDS OVER LAND ON SATELLITE IMAGES

Françoise Désalmand, André Szantai, Geneviève Sèze and Michel Desbois

Laboratoire de Météorologie Dynamique, Ecole Polytechnique,
91128, Palaiseau, France

ABSTRACT

Detecting and tracking low clouds over land is very difficult due to their size and lifetime, below the spatial and temporal resolutions of current imagers and due to the presence of underlying surface features. Improvements are observed with a shorter time interval between images and a better spatial resolution. The influence of different elements has been investigated to increase the retrieval of low-level cloud motion winds (CMWs) over land: the grid size, a reduction of the time interval between images, the use of smaller target areas. A method based on optical flow is used to calculate dense vector fields. The LMD cloud classification has been used to check the level of CMWs extracted with an IR brightness temperature threshold and identified as low-level.

1. Introduction

Preliminary results of the present study have been presented during the 5th International Winds Workshop (Lorne, Australia) (Szantai et al., 2000). New and complementary results from Meteosat-6 and Meteosat-7 images are shown here:

- the effect of different sizes of the target and mesh sizes;
- the effect of reducing the time interval between images (from 30 min to 15 min and 7.5 min);
- the differences of low-level CMWs with dense motion vectors calculated with an optical flow method;
- the verification of the level of CMWs identified as low-level winds by an IR brightness temperature (BT) threshold, with the help of the LMD (Laboratoire de Météorologie Dynamique) cloud classification.

2. Methodology

Cloud motion vectors (CMVs) are generated automatically from a triplet of images, and computed with the Euclidean distance (or sum of squared differences) method, which gives similar or close results to the operationally used cross-correlation method (Leese et al., 1971; Schmetz et al., 1993). Quality tests and tests on the IR BT help to select CMWs at low-level (IR BT above 0°C for the 10 % coldest pixel of the target window). First results of this method have been obtained on Meteosat-4 images (Désalmand et al., 1999) and have shown the advantage of the VIS channel over the IR channel. But, VIS images can be used only between 9:00 and 17:00 UTC, during a third of the day.

3. Target and Grid Sizes

Standard Meteosat-7 images are used in this study (30-min temporal resolution, 2.5-km VIS pixel, 5-km IR pixel). CMWs are computed every 30 min from 09:00 to 17:00 UTC over the whole ten-day period (1-10 August 1998) in the rainy season. VIS images undergo a solar correction to simulate a uniform level of illumination by the Sun, for solar zenithal angles below 75°.

During the rainy season, sub-Saharan Africa is a privileged area to study low clouds over land because of the large extension of the monsoon flow over the continent. At the beginning of August, the monsoon layer is situated in a narrow band between the Guinean gulf (5°N) and the southern edge of the maximal rainfall area of the ITCZ (Intertropical Convergence Zone) at about 15°N (McGregor and Nieuwolt, 1998). Low clouds are in the monsoon layer or just at the top of this layer, or, possibly, between successive convective cells in the ITCZ.

The high resolution (normal) corresponds to a target window of 16*16 VIS pixels (≈ 40*40 km^2) that moves within the search window of 48*48 VIS pixels (≈120*120 km^2). The maximal possible displacement is 16 VIS pixels/30 min (≈ 24 ms^{-1}). Grid-points are separated by 16 pixels (≈ 40 km).
In the case of the low spatial resolution corresponds to a target window of 32*32 VIS pixels (≈ 80*80 km^2) that moves within a search window of 48*48 VIS pixels (≈ 120*120 km^2). The maximal displacement is not modified (16 pixels/30 min ≈ 24 ms^{-1}). Grid-points are separated by 32 VIS pixels (≈ 80 km), and are four times less numerous than for the low spatial resolution.
The maximal speed (24 ms^{-1}) is largely above the monsoon wind speeds measured over West Africa (generally about 5-6 ms^{-1}). So we separate low CMWs with speed below 10 ms^{-1} (about 95%) and CMWs with speed comprised between 10 ms^{-1} and 24 ms^{-1} (5%). These fast CMWs are probably misidentified low CMWs in the vicinity of large convective cells (a well-known problem over the Sahel).

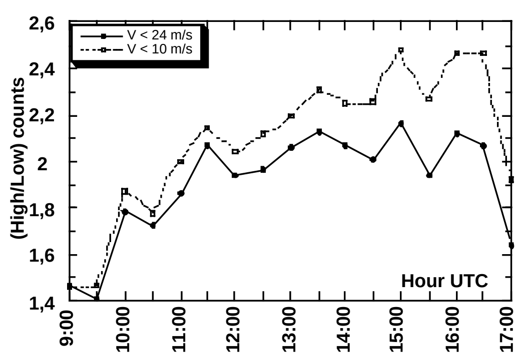

Figure 1. Ratios between high-density counts and low density CMW counts versus time.
Black line: V < 24 ms^{-1}. Dashed line: V < 10 ms^{-1}. Period 1-10 August 1998.

The ratio between the high- and low-density numbers of CMWs is plotted on Figure 1. The advantage of the high-density field is obvious for all low CMWs (ratio comprised between 1.4 and 2) and more particularly for slower ones (ratio comprised between 1.4 and 2.5). However, in spite of four times more numerous grid-points on high density wind fields, we obtain only 1.4 to 2.5 more low-level CMWs in the case of wind speeds limited to 10 ms^{-1}. The reason is that a denser grid cannot increase the number of low clouds present in the cloud field, and that, in many cases, the detection and tracking of low clouds remains very difficult, and even impossible.

4. Impact of Spatial and Temporal Resolutions and Quality Tests

The area of the study is now equatorial East-Africa with the west Indian Ocean coastal area (east Zaire, Uganda, Rwanda-Burundi, Kenya, Tanzania, south Somalia) observed on Meteosat-6 images, on 28 July 1999 from 8:00 to 17:00 UTC.

Three sets of CMWs fields have been computed with:

- time intervals between images of 30, 15 and 7.5 min respectively,
- target windows of 16*16 VIS pixels,
- standard quality tests (temporal and spatial symmetry tests on speed and direction),
- selection of low-level CMWs with the IR BT threshold,

Two other sets of CMWs fields have been computed with:

- time intervals between images of 15 min-,
- small target windows of 8*8 VIS pixels, thus approximately 4 times more vectors are calculated,
- normal or more severe quality tests (symmetry test on direction and spatial consistency tests over a smaller neighbourhood),
- the same selection of low-level winds (same IR BT threshold as in 2.).

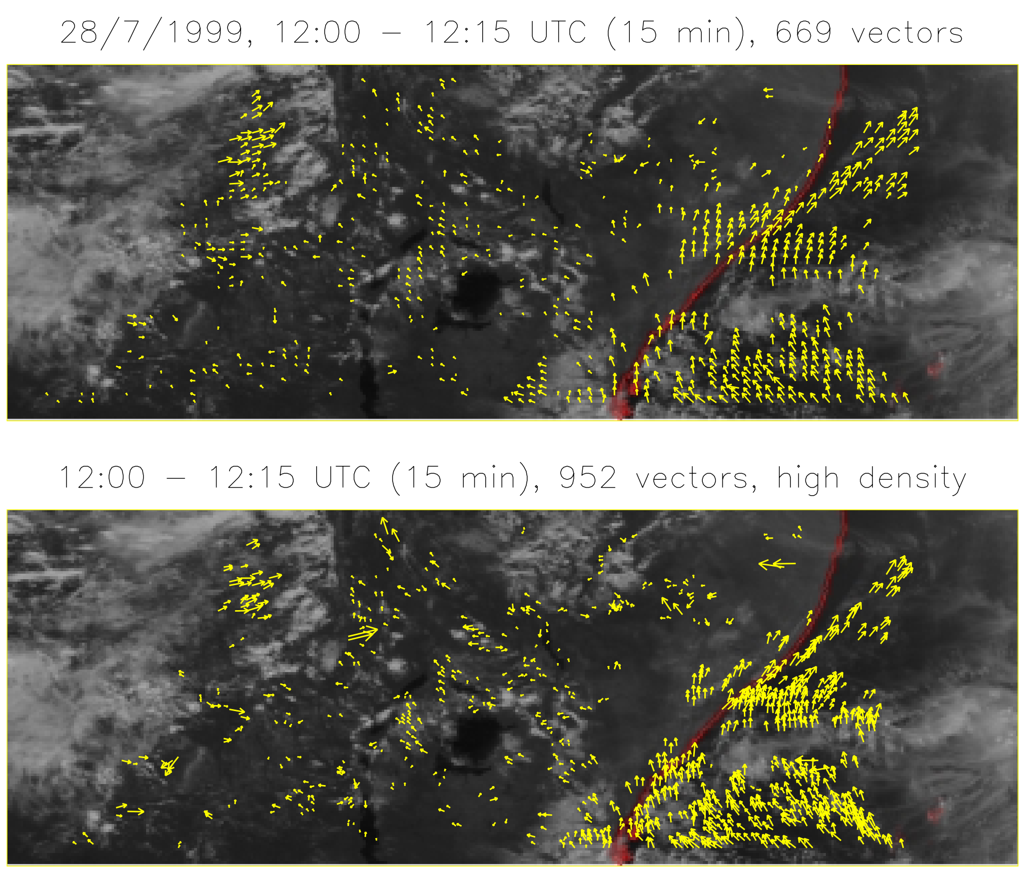

Figure 2.a) and b). Comparison of low-level CMW fields at low and high spatial resolutions, for a time interval of 15 min.

The dramatic increase in the number of vectors is clearly visible when the time interval is reduced from 30 to 15 minutes. When smaller target windows and a denser grid are used, a further increase in the number of vectors can be observed, even with more severe tests. Figure 2 shows the results at 12:00 UTC for 2 cases a time interval of 15 min (the nominal time resolution of the future MSG satellites) with the normal and the high spatial resolution. The ratio between the high and normal spatial resolution numbers is 1.4, in agreement with Figure 1.

Figure 3 shows the evolution in the percentage of vectors (in relation to all grid-points) during the day over land between 8:00 and 17:00 UTC. Important elements are:

- the persisting difference in the percentage of vectors between 30, 15 and 7.5 min,
- an acceptable decrease in the percentage of vectors when high-density CMW fields are calculated (but high-density fields have four times more vectors). Note that the percentages of high density CMWs remain above those for normal density CMWs with a 30-min interval.
- the use of more severe quality tests (difference in direction of 30° instead of 45° for the temporal and spatial consistency tests, a smaller neighbourhood (3*3 instead of 5*5 potential vectors) for the spatial consistency tests) reduces slightly the percentage of CMWs.

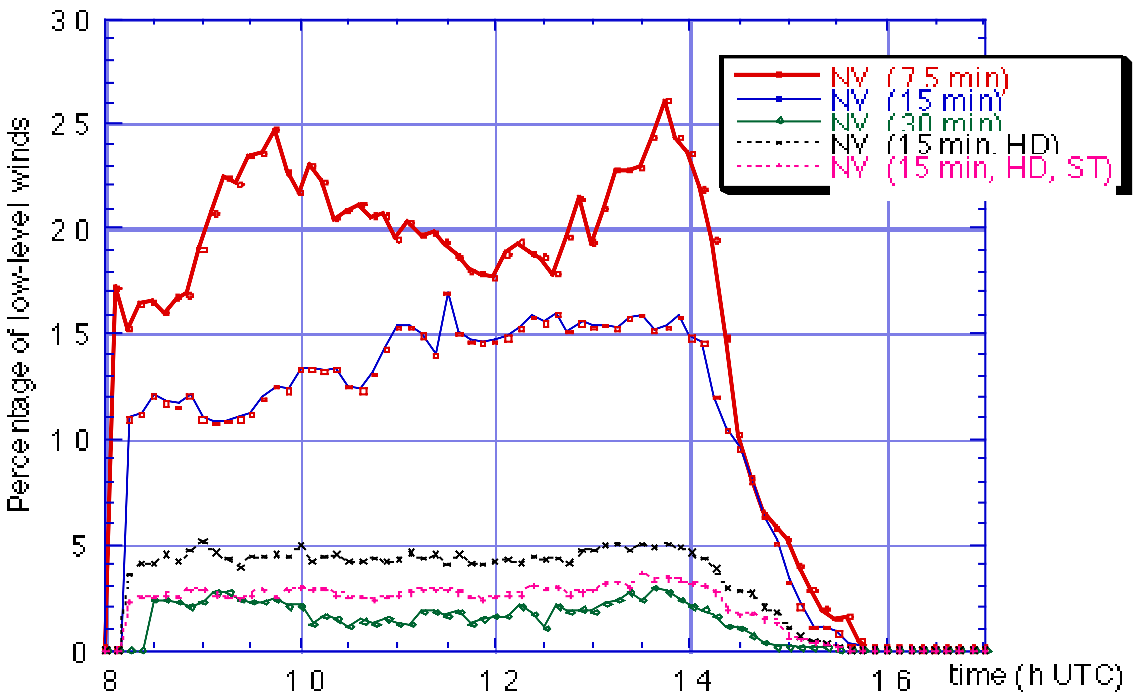

Figure 3. Percentage of low-level CMWS as a function of the time interval between images and spatial resolution (target window size and grid interval), during daytime, over the equatorial East-African area. (100 % correspond to all the 2807 grid points for normal density or to 11111 grid points for high density wind fields.)

5. Comparison of "Classical" Low-Level CMWs and Dense Vector Fields

Two areas, one on the Gulf of Guinea (0-13°E, 1°S-8°N approximately), the other centred on Uganda (23-35°E, 1°S-9°N approximately) have been selected on Meteosat-6 images.

We have compared two sets of motion vectors calculated with different methods:

- cloud motion winds are calculated with a "classical" method, the Euclidean distance method with specific quality tests (2.),
- in dense vector fields, the motion vector of each pixel is basically calculated (Optical flow method - OF). The method is a combination of several techniques used in image processing: a representation (model) of the relation between pixel values and motion vectors (optical flow constraint), the use of robust functions (M-estimators) and a multiresolution-multigrid approach, the introduction of constraints based on divergence and vorticity (Corpetti et al., 2002),
- preliminary results and a more precise description of the methods have been presented during the 5th International Winds Workshop (Szantai et al., 2000).

The average CMW speed is below 5 ms^{-1}. The negative bias (of OF vectors referenced to corresponding low-level CMWs) indicates that CMWs speeds are larger than OF vector speeds. Although the RMS error is small, the normalised RMS error (RMS error/ average of low-level CMW speed) is important, in particular for the Uganda area. Wind directions in both vector fields are similar.

Areas	Bias (ms^{-1})	RMS error (ms^{-1})	Average CMW speed (ms^{-1})	Normalised RMSE
Gulf of Guinea	-0.48	1.50	4.69	32 %
Uganda	-1.48	3.04	4.87	62 %

Table 1. Statistics for the comparison of dense vectors (OF) and CMWs (restricted to land areas).

6. Low-level CMWs Analysed by the LMD Cloud Classification

In order to check the level of CMWs identified as low by the IR BT threshold (2.), the Dynamical Cluster Method (DCM) developed at LMD by Sèze and Desbois is used. A detailed explanation of this clustering method can be found in (Sèze and Desbois, 1987; Sèze and Pawlowska, 2001). Two spectral parameters, the VIS reflectance and the IR BT, with the two associated structural parameters, namely the local spatial dispersion, i.e. the standard deviation computed from the 3x3 pixel values centered on the pixel, are used. For a given region (here West Africa) and a given period (here 1 to 10 August 1998 at 12:00 UTC), the DCM uses the statistical distribution of the four parameters (histogram in the 4-D space of reflectances, IR BT and the two associated local spatial standard deviations) to retrieve cloud and surface types present inside the region area. In the LMD cloud classification, the Meteosat resolution used is the IR resolution (i.e. the VIS is sampled).

On, Figure 4.a, low CMVs have been superimposed to the cloud classification on 1 August at 12:00 UTC. Regions of low winds belong to regions of low clouds in the classification.

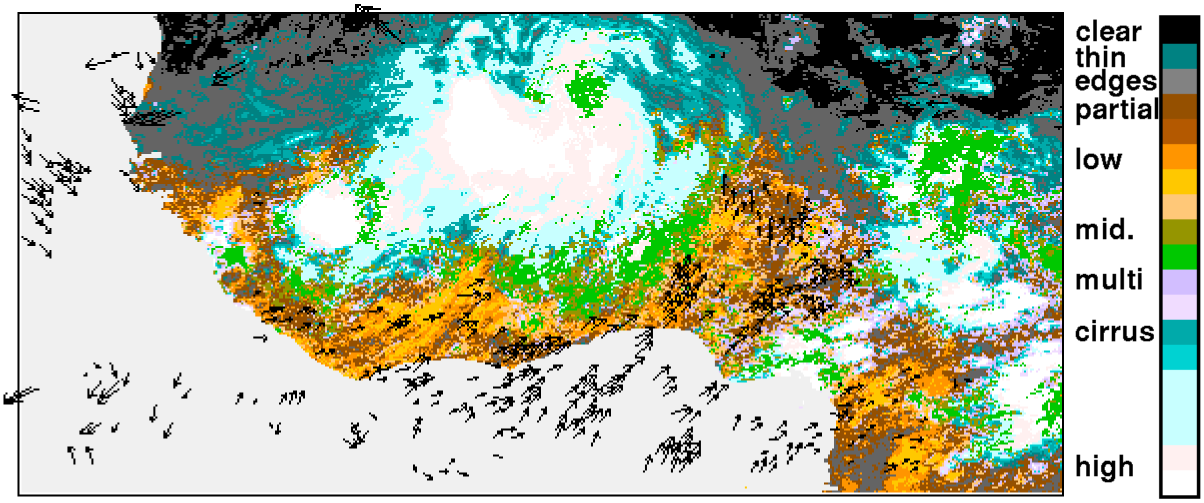

Figure 4.a) Cloud classification and low CMWs for 1 August 1998 at 12:00 UTC

A comparison for the 10-day period of the classifications and the CMWs field is shown on Figure 4.b. The cloud type corresponds to the more frequent cloud type retrieved in a box of 7*7 IR pixels (close to the 16*16 VIS pixels box size used to estimated the wind field) centred on the pixel where a wind is reported. However, when more than 10% of cloudy pixels does not belong to the low cloud class, the CMW is labelled middle or multi-layered or high cloud as a function of the most frequent class among these three types.

- orange bars, in Figure 4.b, give the distribution of the clear and cloud type classes for pixels where a low CMWs is available. This distribution shows that in 78% of the case, low CMWs belongs to regions of low clouds class (57%) or broken low clouds class (21%). The remaining 22% belongs mainly to thin edges class and multi-layered cloud class cases.

➓ -the percentage of middle-high CMWs (IR BT < 0°C) (turquoise bars) in the low clouds classes, is small

➓ -the black bars give for each clear and cloud class the frequency with which a low CMW is available. For a given cloud class, a wind can be estimated in 20% of the case at the most. Low CMWs are more easily estimated in the case of a thick low cloud deck than in the case of broken low clouds.

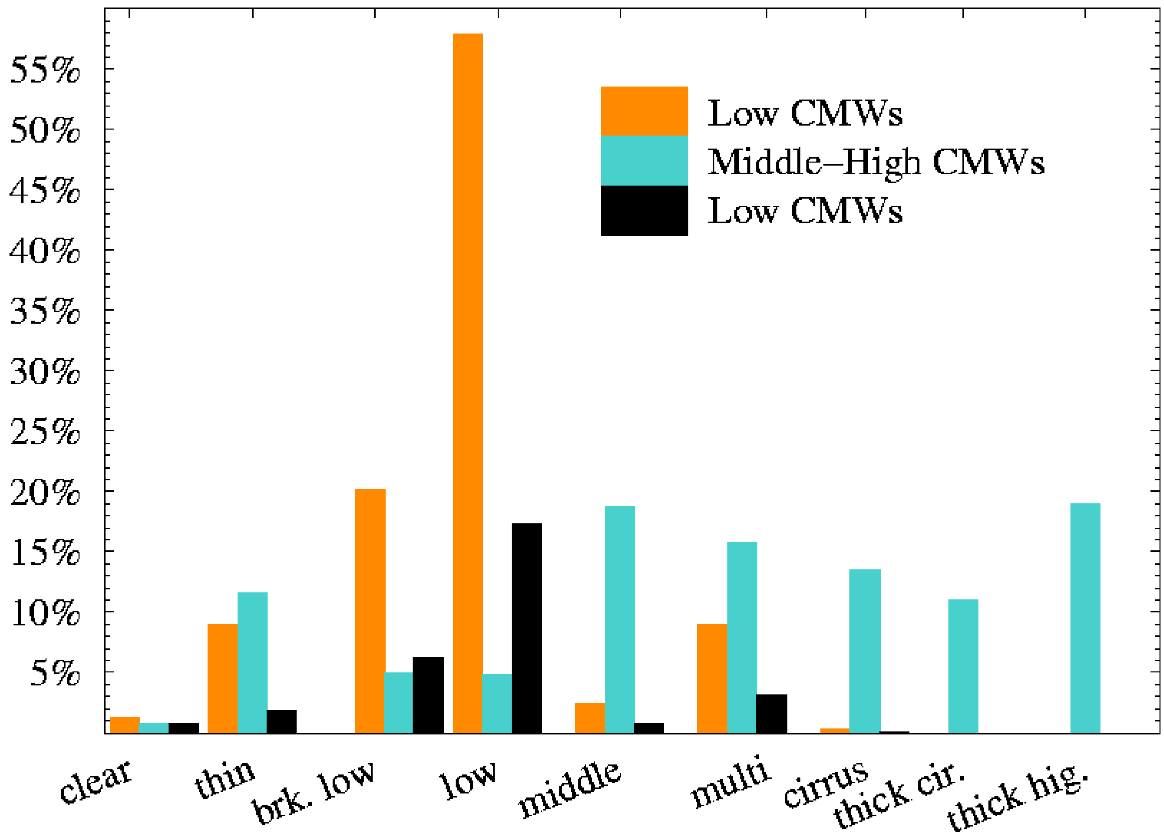

Figure 4.b. Orange bars and turquoise bars: distributions of clear and cloud type classes for the low CMWs and the middle-high CMWs. Black bars: for each clear and cloud type classes, frequency of low CMWs.

In conclusion, low clouds selected by the IR BT threshold of the classical method (2.) are identified as low clouds by the DCM in about 80 % cases. For CMWs belonging to the low cloud class, the frequency of rejection by the IR threshold test is small (3%) More complex cases occur for thin edges of clouds and multi-layered clouds for which the IR BT threshold is not satisfying. For the cloud thin edge class, in 35% of the cases, the wind speed is larger than 10 ms^{-1}.

7. Conclusion and Perspectives

Attempts have been done to improve the retrieval of low CMWs over land, particularly with rapid scans and with a dense grid. A significant increase of the low CMWs have been obtained with the 15-min rapid scan and with a grid mesh of 16-VIS pixels (2.5 km). Comparison between the OF winds and CMWs indicate that OF winds are slower than CMWs and with similar directions. The LMD cloud classification allows to conclude that 80% of low-level CMWs selected by the IR BT threshold of the classical method are found in the low cloud classes; other low clouds probably belong to complex cases, being sometimes « false » low' clouds. For that type of clouds, research is in progress to improve the cloud classification simultaneously with the IR BT threshold. In order to estimate low CMWs at night, attempts are undergoing with the 3.7 µm channel, which will be available on Meteosat Second Generation satellites (MSG).

REFERENCES

Corpetti T., E. Memin, and P. Perez, 2002: Dense estimation of fluid flows. *IEEE Trans. Pattern Anal. Machine Intell*., 23, 3, 365-380.

Désalmand F., A. Szantai and M. Desbois, 1999: An attempt to retrieve low cloud motion winds over land in the African monsoon flow on Meteosat pictures, *Geo. Res. Lett*., 26, n°3, 319-222.

Leese, J.A., C.S. Novak, and B.B. Clark, 1971: An automated technique for obtaining cloud motion from geosynchronous satellite data using cross correlation, *J. Appl. Meteor*., 10, 118-132.

McGregor G. R. and S. Nieuwolt, 1998, Tropical climatology, 2nd Edition, *Ed. John Wiley and Sons Ltd*, 399 p.

Schmetz, J., K. Holmlund, J. Hoffmann, B. Strauss, B. Mason, V. Gaertner, A. Koch, and L. van de Berg, 1993: Operational cloud motion winds from Meteosat infrared images, *J. Appl. Meteor*., 32, 1206-1225.

Sèze, G. and M. Desbois, 1987 : Cloud cover analysis from satellite imagery using spatial and temporal characteristics of the data. *J. Climate Appl. Meteor*., 26, 287-303.

Sèze, G. and H. Pawlowska, 2001: Cloud Cover Analysis with METEOSAT-5 during INDOEX, *J. Geophys. Res*., No. D22, 28, 415-28.

Szantai A., F. Désalmand, M. Desbois, P. Lecomte, P. Perez, S. Zimeras, P. Bouthemy, 2000: Tracking low-level clouds over land on Meteosat images. Proc. Fifth International Winds Workshop, Lorne, Australia (28 Feb. - 3 March 2000). *EUMETSAT*, EUM P28, 245-252.